

Precision Measurement of a Particle Mass at the Linear Collider

C. Milstène¹, A. Freitas², M. Schmitt³, A. Sopczak⁴*

1-Fermi National Laboratory- Batavia-IL-60510 -USA.
EMAIL Address: caroline@fnal.gov

2-Institut für Theoretische Physik, Universität Zürich,
Winterthurerstrasse 190, CH-8057, Zürich, Switzerland.

3- Northwestern University, Evanston, USA.

4- Lancaster University, Lancaster LA1 4YB, United Kingdom.

Precision measurement of the stop mass at the ILC is done in a method based on cross-sections measurements at two different center-of-mass energies. This allows to minimize both the statistical and systematic errors. In the framework of the MSSM, a light stop, compatible with electro-weak baryogenesis, is studied in its decay into a charm jet and neutralino, the Lightest Supersymmetric Particle(LSP), as a candidate of dark matter. This takes place for a small stop-neutralino mass difference.

PACS.14.80, Ly, 85.35+d

1 Introduction

In this study we aim at the minimisation of the systematic uncertainties and of the statistical error [1]. This is achieved by using a method which allows to increase the precision in two ways. We deal with a ratio of cross-sections at two energy points. This takes care of the systematic uncertainties by cancelations and we choose one of the energies to be at the threshold where the sensitivity to mass is maximale. We will show that even though we are dealing with more realistic data than in [2], we improve substantially the precision in the mass measurement. As in [2], we are considering the MSSM with R Parity conservation and a scenario in which a light stop co-annihilates with the Lightest Supersymmetric Particle (LSP), the neutralino, to produce the right amount of dark matter relic density, namely, within the experimental precision of WMAP and the Sloan digital sky survey [3]. Together with a light Higgs, a light right-handed stop also supports electroweak baryogenesis. Our data now include hadronization and fragmentation of the stop before its decay as well as fragmentation of the charm of the decay. This provides a rather big smearing of the particles produced and together with gluon radiation increases the number of jets. We will use two different approaches. First we will optimize a set of sequential cuts as in [2], then we will be using a multi-variable optimization of the neural-network type, the Iterative Discrimination Analysis(IDA). We do take also advantage of the polarization since we deal with an almost right-handed stop as required for E.W. baryogenesis. This allows us to enhance the signal while getting rid of a big part of the background.

2 Mass Precision Measurement: the Method

- The production cross-section of stop pairs $e^+e^- \rightarrow \tilde{t}_1 \tilde{t}_1^*$ is represented to next to leading order (NLO), as a function of the energy for two hypothetical values of the

*presented by A. Sopczak

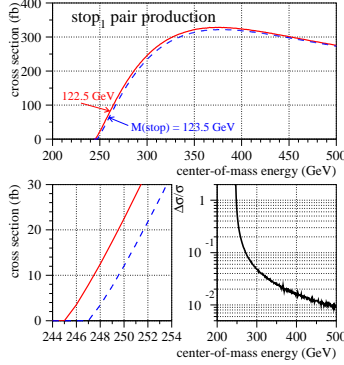


Figure 1: Precision in Pair Production Cross-Section

stop mass, 122.5 GeV and 123.5 GeV, shown in Figure 1.

- In the lower left figure the scale has been blown up and one can see that the sensitivity to small mass difference is high at or close to threshold while in the lower right figure one sees that it is not the case at peak value.
- We will define a parameter Y , as a ratio of production cross-sections at two energy points. This will reduce the systematic uncertainties in Y from the efficiencies as well as from the beam luminosity measurements between the two energy points.
- One of the energy points is chosen at or close to the production energy threshold. This provides an increased sensitivity of Y to mass changes.

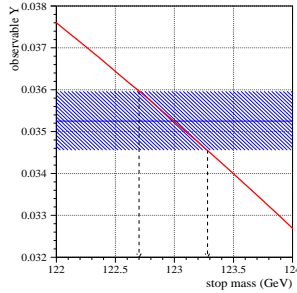


Figure 2: Precision in Determination of the Stop Mass

$$Y(M_X, \sqrt{s_{th}}) \equiv \frac{N_{th} - B_{th}}{N_{pk} - N_{pk}} = \frac{\sigma(\sqrt{s_{th}})\epsilon_{th}L_{th}}{\sigma(\sqrt{s_{pk}})\epsilon_{pk}L_{pk}} \quad (1)$$

σ is the cross-section in [fb], N the number of detected data, B is the number of estimated background events, s is the square of the center of mass energy, ϵ the total efficiency and

acceptance and L is the integrated luminosity. The suffix (th) is used for the point at energy threshold and (pk) for the energy peak. M_x is the mass to be determined with high precision.

As an example, one assumes 3% precision for Y. The blue hashed region represents our measurements. One obtains a precision $\Delta M_x \pm 0.2\%$, the 2 vertical arrows.

In the method, we determine the stop mass by comparing Y with the theoretical calculation of the cross-sections to next to the leading order (NLO) for both QCD and QED. It has been done for +80% polarizations for the e^- beam and -60% polarization for the e^+ beam.

3 The Channel Studied $e^+e^- \rightarrow \tilde{t}_1 \tilde{t}_1^* \rightarrow cX^0 \bar{c}\bar{X}^0$

A scan in the super-symmetry parameter space [5] has shown that a stop mass of 122.5 GeV and a neutralino mass of 107.2 GeV are consistent with baryogenesis and dark matter. The process and the background channels are listed below with their cross-sections with and without polarization.

Process	Cross-section [pb] at $\sqrt{s} = 260$ GeV			Cross-section [pb] at $\sqrt{s} = 500$ GeV		
	0/0	-80%/+60%	+80%/-60%	0/0	-80%/+60%	+80%/-60%
$P(e^-)/P(e^+)$	0.032	0.017	0.077	0.118	0.072	0.276
$\tilde{t}_1 \tilde{t}_1^*$	16.9	48.6	1.77	8.6	24.5	0.77
W^+W^-	1.12	2.28	0.99	0.49	1.02	0.44
ZZ	1.73	3.04	0.50	6.14	10.6	1.82
$We\nu$	5.1	6.0	4.3	7.5	8.5	6.2
eeZ	49.5	92.7	53.1	13.1	25.4	14.9
$q\bar{q}, q \neq t$	0.0	0.0	0.0	0.55	1.13	0.50
$t\bar{t}$	786			936		
2-photon $p_t > 5$ GeV						

Table 1: The Cross-sections at $\sqrt{s} = 260$ GeV and $\sqrt{s} = 500$ GeV for the signal and Standard Model background are given for different polarization combinations. The signal is given for a stop mixing angle of 0.01 and for a stop of $m_{\tilde{t}} = 122.5$ GeV, consistent with E.W. baryogenesis. The e^- negative polarization values refer to left-handed polarization and positive values to right-handed polarization.

3.1 Simulations Characteristics

The signal and background channels were generated with Pythia(6.129), the simulator Simdet(4.03) and for the beamstrahlung Circe(1.0)[6]. They were generated in proportion with their cross-sections.

- Hadronization of the \tilde{t}_1 quark and the fragmentation of the charm quark come from the Lund string fragmentation model. We use Peterson fragmentation [7].
- The stop Hadronization and fragmentation are simulated using T. Sjostrand's code as described in detail by A.C.Kraan[7]. The stop quark is set stable until after fragmentation, then it is allowed to decay. The stop fragmentation parameter is set relative to the bottom fragmentation parameter $\epsilon_{\tilde{t}} = \epsilon_b m_b^2 / m_{\tilde{t}}^2$ and $\epsilon_b = -0.0050 \pm 0.0015$. Later improvements at LEP and a factor two improvement assumed at ILC leads to $\Delta\epsilon_{\tilde{t}} = 0.6 \times 10^{-6}$, as detailed in [8]. The charm fragmentation is set from LEP to $\epsilon_c = -0.031 \pm 0.011$.

- The mean jet multiplicity increased for the data with fragmentation included.

4 The Analysis

The ntuple analysis code [9] which incorporates the Durham jet algorithm is used. The pre-selection and selection cuts are described in detail at both energies in [8]. For a right-handed stop, a run with right-chirality is favorable as shown in Table 1, one expects at 500 GeV a luminosity of 200 fb^{-1} out of the 500 fb^{-1} . The luminosity of 200 fb^{-1} is used for the 0/0 beam polarization as well as a point of comparison.

4.1 The sequential cuts

Were made as similar as possible at the two energies to aim at the cancellation in Y of the systematics. The cuts and their detailed results are given in [8]. In this analysis we allow two, three or four jets with the request that $E_{j25} \geq 25 \text{ GeV}$ for the lowest energy jets. The charm tagging is extracted using the ZVTOP software. The product of Charm tagging of the two jets with the biggest charm probability is used to separate the signal from its main background, since the $We\nu$ has at most one charm jet, whereas the signal has two charm-jets. The backgrounds and the signal efficiencies are shown at the two energies after the sequential cuts in Table 2.

4.2 Iterative Discriminant Analysis (IDA)

Combines the kinematic variables in parallel. The same kinematical variables and simulated events are used than in the cut-based analysis. A non-linear discriminant function followed by iterations enhances the separation signal-background. Both signal and background have

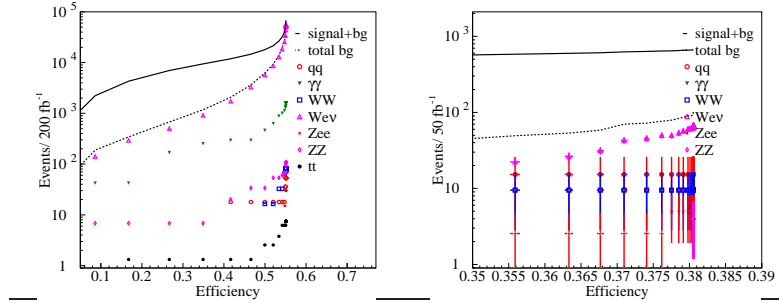


Figure 3: Detection Efficiency and Background Events at 500 GeV(left) and 260 GeV (right).

been divided in equally sized samples, one used for the training, the other as data. We will make two IDA iterations in our final analysis [8]. The results are shown after a first IDA iteration for which one keeps 99.5% of the signal efficiency followed by a second iteration. We assume the same luminosities and polarizations than for the sequential based analysis. The results are in Table 2. The events $< N$ show the number of events corresponding to a single event.

	$\mathcal{L} = 50 \text{ fb}^{-1}$, at 260 GeV			$\mathcal{L} = 200 \text{ fb}^{-1}$, at 500 GeV			$\mathcal{L} = 50 \text{ fb}^{-1}$, at 260 GeV		$\mathcal{L} = 200 \text{ fb}^{-1}$, at 500 GeV	
	Sequential Cuts			Sequential Cuts			IDA		IDA	
Pe^-/Pe^+	generated	0/0	Pol+	generated	0/0	Pol+	0/0	Pol+	0/0	Pol+
$t_1 t_1^*$	50,000	544	1309	50,000	5170	12093	619	1489	9815	22958
W^+W^-	180,000	38	4	210,000	16	2	11	1	<8	<1
ZZ	30,000	8	7	30,000	36	32	<2	<2	20	18
$We\nu$	210,000	208	60	210,000	7416	2198	68	20	1719	510
eeZ	210,000	2	2	210,000	<7	<6	3	2	<7	<6
$q\bar{q}, q \neq t$	350,000	42	45	350,000	15	17	16	17	18	21
$t\bar{t}$		-	-	180,000	7	7	-	-	1	1
2-photon	1.6×10^6	53	53	8.5×10^6	12	12	27	27	294	294
Total Background		351	171		7509	2274	127	69	2067	851
S/B		1.5	7.6		0.7	5.3	4.9	22	4.7	27
Efficiency		0.340			0.212		0.387		0.416	

Table 2: Signal and background generated to NLO and after selection cuts are shown at $\sqrt{s} = 260 \text{ GeV}$ and 500 GeV , for total luminosities of 50 fb^{-1} and 200 fb^{-1} , respectively and the signal efficiencies. The event numbers after selection cuts are given without and with beam polarization. $Pol+ = Pe^-/Pe^+$ for $Pe^- = +80\%$ and $Pe^+ = -60\%$.

4.3 Contributions to the Mass Uncertainties

In Table 3 is summarised the contributions to the mass uncertainties

Error source for Y	Cut-based analysis	Iterative Discriminant Analysis
Detector effects(systematics)	0.9%	2.4%
Charm fragmentation (systematics)	0.6%	0.5%
Stop fragmentation(systematics)	0.7%	0.7%
Neutralino Mass(systematics)	0.8%	2.2%
Background Contribution(systematics)	0.8%	0.1%
Sum of experimental systematics	1.7% ($\Delta m_{\tilde{t}_1} = 0.10 \text{ GeV}$)	3.4% ($\Delta m_{\tilde{t}_1} = 0.21 \text{ GeV}$)
Statistical	3.1% ($\Delta m_{\tilde{t}_1} = 0.19 \text{ GeV}$)	2.7% ($\Delta m_{\tilde{t}_1} = 0.17 \text{ GeV}$)
Sum of experimental errors	3.5% ($\Delta m_{\tilde{t}_1} = 0.24 \text{ GeV}$)	4.3% ($\Delta m_{\tilde{t}_1} = 0.28 \text{ GeV}$)
Theory for signal cross-section	5.5%	5.5%
Total error ΔY	6.5% ($\Delta m_{\tilde{t}_1} = 0.42 \text{ GeV}$)	7.0% ($\Delta m_{\tilde{t}_1} = 0.44 \text{ GeV}$)

Table 3: Combination of statistical and systematic errors for the determination of the stop mass from a threshold-continuum cross-section measurement. In parenthesis is given the overall error on the measured mass. An beam spectrum error $\Delta m_{\tilde{t}_1} = 0.1 \text{ GeV}$, is included.

The next to next to leading order (NNLO) QCD corrections are expected to be of the same order than the NLO. This is based on the top quark results. Assuming a factor two improvement in the calculations by the time ILC is running (A 1% NNLO correction is also included for the EW component). The relic dark matter density is shown below

5 Conclusions

We deal with more realistic data, including quarks hadronization and fragmentation, and with a lower integrated luminosity, almost by a factor two, but still manage to improve the stop mass precision by a factor three comparatively to [2]. The results of the dark Matter

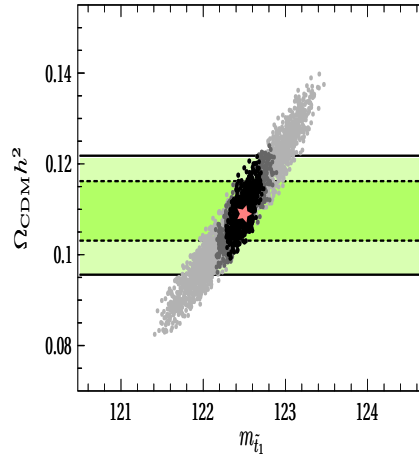


Figure 4: Dark matter Relic Density

relic density versus the stop mass precision are shown in three cases, in the last figure. The light grey dots represent our previous results[2] for $\Delta m_{\tilde{t}_1} = 1.2$ GeV, the dark grey dots correspond $\Delta m_{\tilde{t}_1} = 0.42$ GeV, $\Omega_{CDM}h^2 = 0.109+0.015-0.013$, include both experimental and theoretical errors. The black dot imply $\delta m_{\tilde{t}_1} = 0.24$ GeV . $\Omega_{CDM}h^2 = 0.109+0.0012-0.0010$, experimental errors sequential cuts. It is only a small improvement in the precision of the dark matter density with respect to $\Delta m_{\tilde{t}_1}=0.42$. The red star is our working point. The precision is very comparable to $0.103 < \Omega_{CDM}h^2 < 0.116$, the current WMAP results are shown by the horizontal green bands on the figure for 1σ and 2σ constraints.

References

- [1] Slides:
<http://ilcagenda.linearcollider.org/contributionDisplay.py?contribId=49&sessionId=69&confId=1296>
- [2] M. Carena, A. Finch, A. Freitas, C. Milstene, H. Nowak, A. Sopczak, Phys. Rev.**D72** 115008 (2005). C. Milstène, M. Carena, A. Finch, A. Freitas, H. Nowak and A. Sopczak, in *Proc. of International Workshop on Linear Colliders (LCWS 2005), Stanford, California, 18-22 Mar 2005* [hep-ph/0508154]; C. Milstène, M. Carena, A. Finch, A. Freitas, H. Nowak and A. Sopczak, in *Proc. of International Linear Collider Physics and Detector Workshop, Snowmass, Colorado, 14-27 Aug 2005*, eConf C0508141.
- [3] D. N. Spergel *et al.* [WMAP Collaboration], astro-ph/0603449. M. Tegmark *et al.* [SDSS Collaboration], *Astrophys. J.* **606**, 702 (2004).
- [4] G. Feldman, R. Cousins, Phys. Rev.**D57**3873 (1998).
- [5] C. Balazs, M. Carena, C. Wagner) hep-ph/0403224v2-(2004).
- [6] T. Sjöstrand, P. Eden, C. Friberg, L. Lönnblad, G. Miu, S. Mrenna and E. Norrbin, *Comput. Phys. Commun.* **135**, 238 (2001); see also T. Sjöstrand, L. Lönnblad and S. Mrenna, and hep-ph/0108264. (Pythia). M. Pohl and H. J. Schreiber, hep-ex/0206009, (Simdet). T. Ohl, *Comput. Phys. Commun.* **101**, 269 (1997), (Circe).
- [7] T. Sjöstrand, <http://www.thep.lu.se/~torbjorn/pythia/main73.f.html>. Peterson *et al.* Phys. Rev.**D27** 105 (1983), (Petersen). A. C. Kraan, *Eur. Phys. J. C* **37**, 91 (2004).
- [8] A. Freitas, C. Milstene, M. Schmitt, A. Sopczak. arXiv:0702.4010
- [9] T. Kuhl, *N-Tuple working on Simdet DST structure*, <http://www.desy.de/~kuhl/ntuple/ntuple.html>.